SARAF 4-ROD RFQ RF POWER LINE SPLITTING DESIGN AND TEST

J. Rodnizki†, B. Kaizer, Z. Horvitz, L. Weissman, A. Perry, D. Hirschmann, Soreq NRC SARAF, Yavne, Israel

Abstract

The SARAF 3.8 m long 4-rod RFQ is able to accelerate 4mA CW proton beam to 1.5 MeV. During the last years several experiments with CW proton beam up to 2 mA and in the range of 1.9– 4 MeV were run at SARAF linac. The conditions for running CW deuteron beams (250 kW CW dissipated power or a 65 kV inter-rod voltage) have not been achieved yet. Our findings imply that the RFQ coupler was the primary bottle neck. Thus, a project to split the RFQ power line was initiated. In the framework of the project, a 3 dB splitter and two new RF couplers were installed. The RF couplers were manufactured in-house according to an improved design which included better brazing methods and better vacuum and RF sealing. This project is innovative from two points of view: (a) Implementation of two couplers located in two separated RF cells in a 4-rod RFQ. Synchronization of the incident power phase in both couplers was achieved by a single LLRF control channel and phase matching was achieved by adjusting the length of the RF rigid lines. (b) RFQ availability at 200 kW CW was demonstrated. This power range is sufficient for acceleration of a high intensity 5 mA CW deuteron beam to 1.3 MeV/u by a new modulation of the RFQ rods. To our knowledge, SARAF RFQ will be the first 4-rod RFQ capable of running a CW deuteron beam.

INTRODUCTION

The SARAF 176 MHz, 3.8 m long 4-rod RFQ is able to generate a 1.5 MeV 4mA CW proton beam. During the last few years, several experiments with CW proton beam up to 2 mA and in the range of 1.9 – 4 MeV were run at SARAF linac, [1, 2]. In order to run a CW deuteron beam the required RFQ power is 250 kW CW, to reach a 65 kV inter-rod voltage. This amounts to four times the power needed to run a CW proton beam. The maximum reachable value demonstrated few times in recent years, was around 200 kW in CW operation mode using a single RF coupler. In 2014 an extensive conditioning campaign of the SARAF RFQ has achieved stable operation in CW mode for 4.5 hours at 200-205 kW incident power and 50% duty cycle pulsed mode at 250 kW [3]. However, these capabilities could not be maintained for extended times. During 2015, several events of copper evaporation on the ceramics in the coupler RF window were occurred and we could not bring the RFQ back to the same operational level. It became evident that the status of the RF coupler has deteriorated and as a result deuteron beam operation was not possible. Subsequently, it was decided to replace the original single coupler with two improved couplers and to split the coaxial line from the amplifier, as a complementary step to the RFQ improvements reported in [4]. The goal of the project was to reduce the RFQ coupler load and, hence, achieve long term stable operation of the current RFQ.

A proposal for redesign the SARAF RFQ rods with purpose to reduce the integrated RFQ load required for deuteron operation was also under consideration [5]. Defining the available upper limit of this load with the new improved couplers system was another important objective of this work.

THE COUPLERS AND RF SYSTEM

General Layout

The project included installation of a 3 dB RF splitter at 176 MHz (the linac frequency), new RF lines structure and two new upgraded couplers with individual directional couplers (Fig. 1). The 3 dB splitter was adopted due to its ability to isolate crosstalk between the two couplers in order to enable a stable beam operation. The available RF power (up to 300 kW) was split towards the two couplers. A dummy load that is able to absorb 150 kW from the reflected power was connected to the port next to the injected forward power.

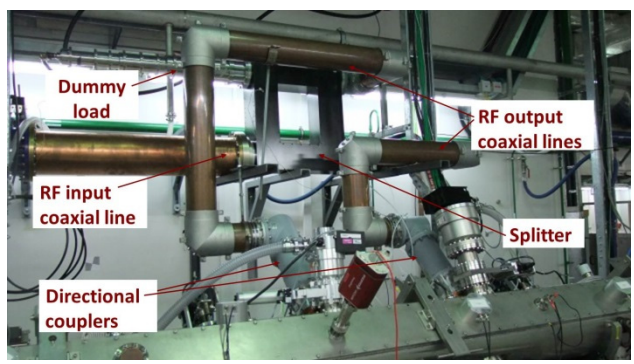

Figure 1: Configuration of the RF lines.

Phase Matching Between Both Couplers Ports

The magnetic phase between adjacent RF cells (total 40 stems along the RFQ with 39 RF cells) is 180º. The shift is due to the eigenmode pattern of the magnetic field, induced by the coupler (Fig. 2). As a result the relative phase between the couplers loops is 180º due to the odd number of RF cells between them.The output ports of the 3 dB splitter have 90º phase shift. By extending the length of the RF line by 1/4 λ the requirded phase matching between the two couplers port is achieved to within a deviation of ~1º, equivalent approximately to a 5 mm deviation in the rigid RF line length. The superposition of the combined induced fields from both ports on the excited RFQ eigenmode may be evaluated by:

$$A\cos(wt-\alpha/2)+A\cos(wt+\alpha/2) = 2A\cos wt\cos\alpha/2$$

† jacob@soreq.gov.il

ISBN 978-3-95450-169-4

where A is the amplitude of the induced matgnetic field at each port and α is the phase shift deviation between the ports from the specified 180º.

In our case, the phase shift deviation is 1º. The reduced injected forward power, normalized to injection through one coupler, will be proportinal to the amplitude field square: $\cos^2(\alpha/2) = 0.9999$. Thus net relative reduction in the forward power to the RFQ as a result of the phase mismatch is negligible.

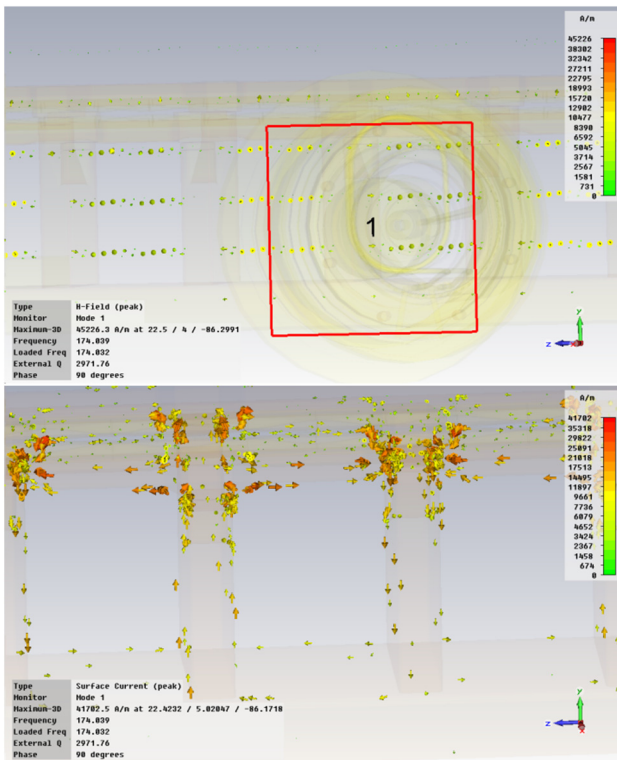

Figure 2: The eigenmode induced magnetic field by the coupler at 176 MHz (top) and the generated surface currents (bottom).

RF Study of the Coupler Loop

The RFQ coupler loop has to be adjacent to the RFQ stems electrodes and the base plate. In general, the coupling may be achieved by a loop oriented normally to the induced magnetic field of the generated eigenmode. The two available configurations are: (a) the loop is normal to the rods structure (b) the loop is parallel to the rods structure (Fig. 3, 4). Both configurations were considered for SARAF RFQ. The Q_0 of the SARAF RFQ is of the order of 4000. This requires that the $Q_{external}$ of an individual coupler to be close to 8000.

The results of simulations for the normal plane coupler configuration are shown in Fig. 3. The electric (Fig. 3 left) and magnetic (Fig. 3 right) fields are shown for distance of 4 mm and 6 mm, respectively, between the loop and a stem. The calculated external Q values were10640 and 9470 for a 6 mm and 4 mm distances correspondingly. It was not possible to achieve the required coupling at this configuration.

The results of simulations for the parallel plane configuration are shown in Fig. 4. The electric (Fig. 4 left) and magnetic (Fig. 4 right) fields are shown for the distances of 6 and 4 mm correspondingly between the loop and the stems. The obtained external Q values were 7530 and 6460 for distances of 6 and 4 mm respectively. Thus, the required coupling (8000) is achievable by fine tuning of the coupler position. The parallel plane configuration was selected for production. The final loop coupling for this antenna shape is tuned by bending and gives the required coupling.

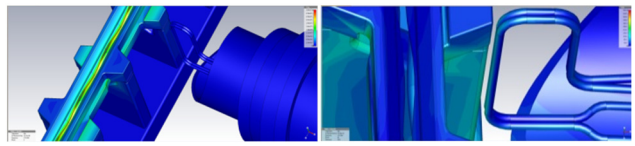

Figure 3: Normal plane loop configuration.

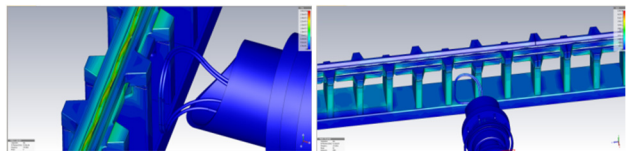

Figure 4: Parallel plane loop configuration.

Coupler Loop Engineering Design Considerations

The old RF coupler loop included two copper water cooled tubes which were silver brazed (Fig. 5). The silver brazing material includes light elements which might immigrates to the vacuum during operation. In the new design the two copper tubes were not brazed and about 4 mm space was kept between them along the whole length. The only place of brazing was at the vacuum water feedthroughs. The brazing was done with CuSil material [6] which is widely recommended for accelerator components [7]. The brazing to the water feedthrough was performed only after the first order tuning procedure of the couplers was accomplished when the couplers legs lengths were determined (see below). Helium leak test was performed after the coupler brazing.

Figure 5: The former design of the coupler (left) and the upgraded coupler (right).

The new design (Fig. 6) includes the following features: RF canted springs were adopted for RF contact to avoid phenomena like RF broken fingers and loose RF contacts at the former design (Fig. 5). The RF contacts were applied via the RF springs only. Drilled channels were used to avoid the virtual leaks which occurred in the former design. The required tolerance in the new design between the coupler base assembly components guaranteed the adequate space for possible thermal expansion.

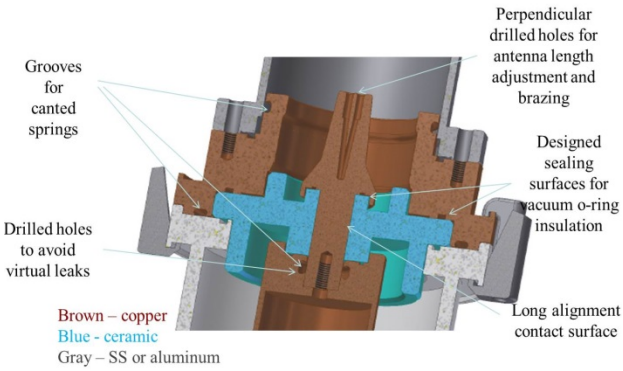

Figure 6: The upgraded assembly improvements.

The Matching of Both Couplers to the RFQ

The matching of one coupler is relatively easy to achieve. One may vary the coupling loop position by translation or rotation (depending on the coupler configuration) with the goal of reaching the minimal reflected power. It is more complicated to match two couplers simultaneously. At the first stage the couplers were matched one at a time while the second coupler was not installed. The matching procedure for each coupler was based on two consecutive steps:

(a) Applying network analyser the coupler loop position was adjusted iteratively to the minimal reflected power (expected value -40 dB). The quality factor Q_{load} was measured. (b) Next the coupler loop position was modified to reach $Q'_{load}=4/3Q_{load}$. Then both couplers were assembled together, the expected loaded quality factor for this configuration was the original Q_{load}. After fine tuning of the both couplers a preliminary critical coupling was achieved for the entire system. The brazing of the couplers to the water feedthroughs (see above) was done only at this moment. Eventually, the final tuning of the entire mounted system was performed by gentle adjustment of the loops while minimizing the reflected power of each of them.

The final step of the coupler tuning is illustrated in Fig. 7. One can notice that S_{21} (the ratio between the RFQ pickup power to the injected forward power) demonstrated a non-symmetric behaviour around the critical coupling. This was probably due to the nonstandard design of the loop as the inner and outer cooling tubes were not brazed along the loop. However, as is demonstrated in the figure, S_{11} (the ratio between injected to reflected powers) had a good response with negligible losses.

The Modified RF System

The upgraded RF diagram for the two coupler configuration is shown in Fig. 8. A careful matching of the RF lines after the splitter (see above) ensured that the RFQ response to the forward power was similar to the response in the previous configuration. The reflected power was fully reflected back to the amplifier as in the former configuration. This occurred due to the 90º phase shift between the reflected power signals from the two couplers at the RF splitter. Thus, the LLRF control of the RFQ was not modified. The forward and reflected powers were monitored at each coupler using the corresponding directional couplers. These values were compared with the total forward and reflected powers measured at the exit of the RF amplifier.

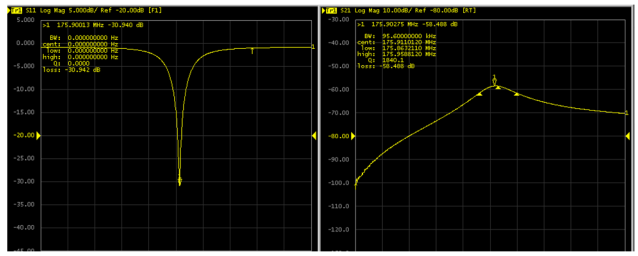

Figure 7: S_{11} (right) and S_{21} (left) during the final tuning stage of the coupler antenna.

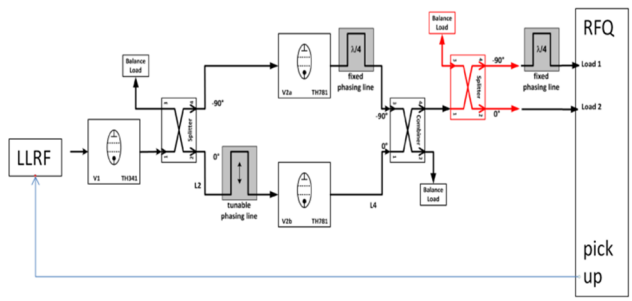

Figure 8: The modified RF system diagram.

THE RFQ CONDITIONING

The RFQ was cleaned prior the RFQ closure and the rods polished with alcohol socked tissue. A few CCD cameras were installed at the viewports in front of the couplers and the rods. A few x-rays detectors were installed in front of the viewports for monitoring x-ray flux. Several thermocouples were attached to the RFQ tank, cooling lines feedthrough interfaces and RF lines. To avoid partial virtual leaks that might lead to field breaks the RFQ conditioning activity was initiated with one week of pumping the RFQ till vacuum pressure of $4.5\cdot10^{-7}$ mbar was reached. During pumping, when cooling water has been cycled through the RFQ, the vacuum improved. This phenomenon was a result of lower degassing rate from the surfaces (see Fig. 9). At the end of the conditioning program the vacuum level reached $2\cdot10^{-7}$ mbar.

The RFQ was carefully brought to the dissipated power of 200 kW CW by keeping a quasi-steady state behaviour of the thermocouples signals during the power ramp. Stable operation was systematically demonstrated for several hours duration with RFQ availability greater than 95%. The reflected power in this range is around 2%. Applying higher dissipated power, an onset of forward and reflected power fluctuations took place (see Fig. 10). Several studies reported vibration of the 4-rods structure at high loads [8]. The RFQ dissipated power exhibited the linear dependence with the square of the RFQ pickup voltage based on CW measurements up to 200 kW CW dissipated power and up to incident power of 250 kW at pulse mode with a maximal deviation from linearity of 4% (see Fig. 11). The deviation from linearity was, most likely, related to field emission and corona currents.

ISBN 978-3-95450-169-4

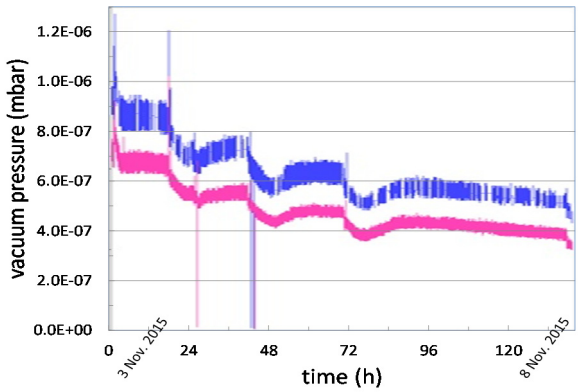

Figure 9: Evolution of the RFQ vacuum level along the first week of the conditioning.

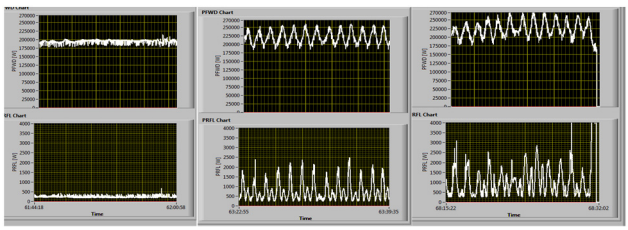

Figure 10: Forward and reflected power oscillations at different power levels (left to right): 200kW (stable), 215kW and 225kW.

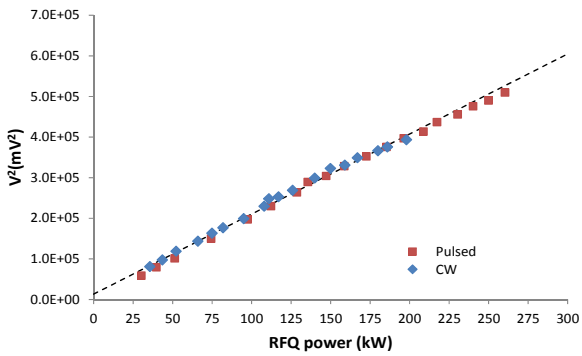

Figure 11: Square pickup voltage as function of forward power for CW and pulse operation.

An eight hour run was performed, testing the availability of the RFQ at 250kW in the pulsed mode. The duty cycle was gradually increased during the test from 50% to 80%, A few hours of conditioning at the lower values of duty cycles preceded this measurement. Data presented in Fig. 12 is corresponded to the situation when operator promptly intervened in the cases of RFQ trips.

DEUTERON BEAM OPERATION

The deuteron beam operation following the conditioning campaign was run at pulse mode with significance duty cycle of the RFQ (around 30%) and small beam duty cycle (around 1%) to enable use of destructive beam diagnostics. The tests consisted of: measuring the beam energy by Time of Flight (TOF) (see Fig. 13) and by the Rutherford back scattering (RBS) of deuterons towards a silicon detector (see Fig. 14). Both measurements yielded the beam energy of 1.50±0.01 MeV/u. The MEBT BPM signals, for 8.5 mA deuteron beam injected to the RFQ, as a function of forward power are shown in Fig. 15.left. The lower signal amplitude measured at BPM1 is due to the bunch spread, since BPM1 is downstream of BPM2. Beam transmission measurements as a function of forward power are shown in Fig. 15.right for 4.5 mA and 8. mA values of the injected deuteron current. The slightly better beam transmission for higher current is probably due to its lower transverse emittance upstream the RFQ. It is not clear why the maximum BPM signal corresponds to a RF power higher than the one that corresponds to the optimum transmission. Probably, the better bunching was achieved at these RF values. The forward power needed to achieve optimal beam transmission at the desired beam energy, around 250 kW, is similar to the spent forward power for one coupler configuration. One can conclude that the dissipated power is spent on the desired RFQ eigenmode with low losses for dark currents and a small percentage returned as a reflected power.

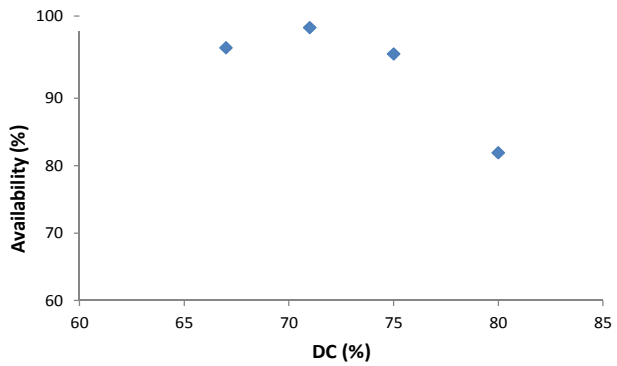

Figure 12: Dependence of the RFQ availability at 250 kW for high values of duty cycle.

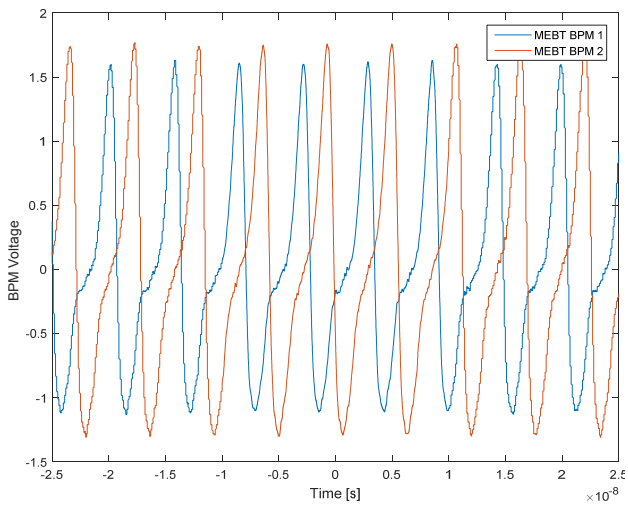

Figure 13: TOF measurement between the MEBT BPMs confirmed that the deuteron energy downstream the MEBT is 1.5±0.1 MeV/u.

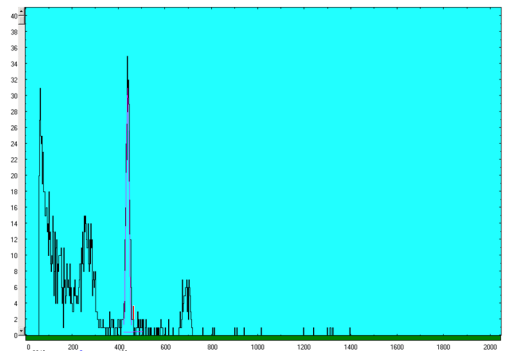

Figure 14: RBS measurements of deuteron energy distribution approved that the mean beam energy is 1.50±0.01 MeV/u. Peak at channel 430 corresponds to Rutherford scattering deuterons off the gold foil

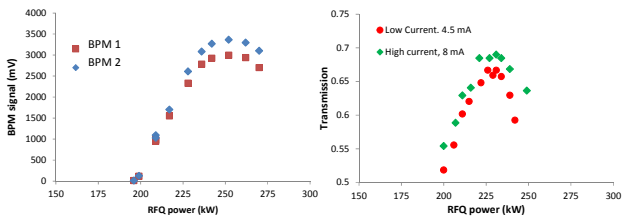

Figure 15: Left- MEBT BPMs amplitude as a function of RFQ forward power for 8.5 mA LEBT injected current. Right- RFQ transmission of deuteron beams as a function of RFQ power.

Beam transmission as a function of the injected LEBT currents is shown for a proton and a deuteron beams in Fig. 16. In this figure it is demonstrated that a 5.5 mA deuteron beam was available at the RFQ downstream end for an 8.5 mA injected beam. It appears that the maximum available proton current downstream the RFQ in the current LEBT configuration was limited to 4 mA. Lower transmission for protons is, probably, due to their higher LEBT emittance.

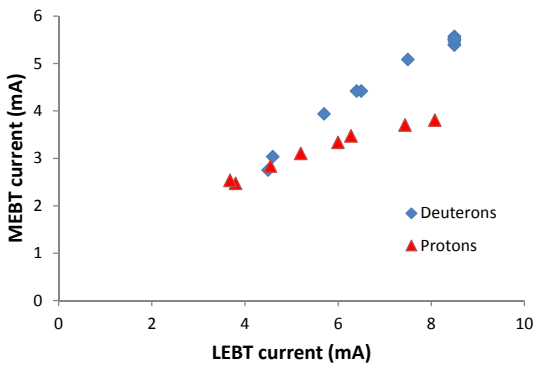

Figure 16: RFQ transmission as a function of injected LEBT current for a proton and a deuteron beams.

The emittance measurements at the SARAF D-plate for a 3.6 mA deuteron beam downstream the RFQ and the PSM are shown in Fig. 17. The rms measured values at the D-plate (0.136, 0.162) normalized transverse emittance, were well below the expected values downstream the RFQ - 0.2 π·mm·mrad. It is worth noting that the emittance is slightly reduced by a beam scrapper placed downstream the RFQ exit.

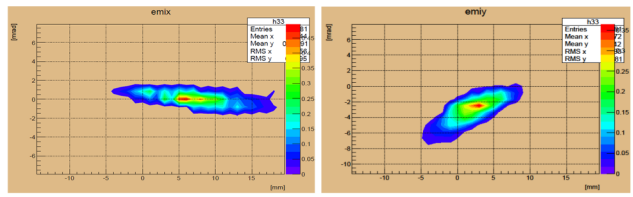

Figure 17: RMS emittance measurements for the 3.6 mA deuteron beam.

SUMMARY

An upgrade of the SARAF RFQ RF system was performed. The existing RF coupler was replaced by two new ones of superior design. The RF coaxial line was split and the RF coaxial sections were adjusted to match phases. The proper RF coupling was achieved successfully by tedious, iterative procedure. The upgrade of the RF system allowed one to improve the RFQ performance and its availability for beam operation. The beam transport of 5.5 mA deuteron beam at RFQ exit was demonstrated. Stable operation at 200 kW CW was demonstrated, allowing one with confidence to launch the next program for modification of the RFQ 4 rod structure. An updated design of the RFQ 4 rods modulation with lower RF load target to 1.3 MeV/u is expected to enable CW operation of the RFQ for a deuteron beam. The splitting of the RFQ 4 rods RF power to two couplers is pioneer project and may contribute to other projects which intend to run CW beams in high power dissipation per meter, like the FRANZ [9] and MYRRHA [10] 4-rod RFQ.

ACKNOWLEDGEMENT

We would like to acknowledge Mr. L. Dadon for the couplers brazing works and Dr. A. Kreisel for his assistance in the beam emittance analysis. We are grateful to the SARAF team for their support during the work on this project and to personal of the Soreq workshop for their assistance during manufacturing and installations phases.

REFERENCES

[1] S. Halfon *et al.*, Appl. Rad. and Isot. 106 (2015) 57–62.

[2] M. Tessler *et al.*, Phys. Lett. B 751 (2015) 418–422.

[3] L. Weissman *et al*, "SARAF Phase I linac operation in 2013–2014", JINST 10 (2015) T10004.

[4] J. Rodnizki *et al.*, "RFQ RF and thermal improvements", SNRC 4716, 2014.

[5] A. Shor and J. Rodnizki, "Redesign of SARAF RFQ rods for CW deuteron acceleration", SNRC 4517 (2014).

[6] http://datasheets.globalspec.com/ds/3022/

[7] S. R. Ghorke *et al.*, XXVI Int. Symp. On Discharges and Electrical Insulations in Vacuum.Mumbai, India, 2014.

[8] D. Koser, P. Gerhard, L. Groening, O. Kester, H. Podlech, IPAC2016, MOPOY020, Busan, Korea

[9] C. Wiesner *et al.*, "FRANZ and small-scale accelerator-driven neutron sources", IPAC'15.

[10] Chuan Zhang, Holger Podlech, IPAC'14, THPME008, Dresden, Germany.

ISBN 978-3-95450-169-4